Supporting Information

Cambronne et al. 10.1073/pnas.1218887109

SI Materials and Methods

miRNA Mimics. Based on mature sequences (hsa–miR-132–3p; hsa–miR-124–3p; hsa-miR-181d-5p; miR–Scrm: AUGUGGUCCA-ACCGACUAAUACAG), dsRNA oligo mimics consisted of 5′ phosphates, 2-nt overhangs at each 3′ end, and a single base pair mismatch at nt 4 from the 3′end of the passenger strand (1). Cel-miR-239b dsRNA oligo mimic was purchased from Dharmacon.

qPCR. A total of 100 ng RNA was used for generation of first-stand cDNA using oligo-dT (T_{15}–T_{20}) following standard SuperScript III manufacturer protocol (Invitrogen). Samples were then diluted 1:15 with water and 2 μL of diluted cDNA was used in triplicate for qPCR with SYBR Supermix (Bio-Rad) and gene-specific primers.

Cell Culture, Transfections, and Antibodies. HEK293T cells were grown in DMEM media supplemented with 10% (vol/vol) FBS. Either Lipofectamine 2000 or calcium phosphate was used to transfect expression vectors for Flag–dnGW182, dual luciferase constructs in pSI–Check2 (Promega), CMV–Flag–PTBP1, and/or microRNA oligo mimics. Primary antibodies used for Western blotting include anti-Flag M2 (Sigma), anti-Ago1 4B8 (Sigma), anti-Ago2 (Abcam; ab57113), anti-GAPDH (Millipore; MAB374), CRK C-18 (SCBT), anti-HbEGF (Abcam; ab16783), anti-TJAP1 (Abcam; ab80444), anti-DHHC9 (Abcam; ab74504), and anti–α-tubulin DM1A (Sigma).

Definition of MREs. Motifs were defined following Baek et al. (2) and Chi et al. (3).

1. Schwarz DS, et al. (2003) Asymmetry in the assembly of the RNAi enzyme complex. *Cell* 115(2):199–208.
2. Baek D, et al. (2008) The impact of microRNAs on protein output. *Nature* 455(7209): 64–71.
3. Chi SW, Hannon GJ, Darnell RB (2012) An alternative mode of microRNA target recognition. *Nat Struct Mol Biol* 19(3):321–327.

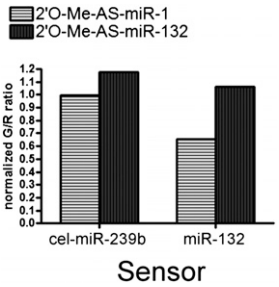

Fig. S1. Detection of endogenous miR-132 activity in HEK293T cells. Bidirectional two-color sensors (1) for miR-132 and control cel-miR-239b were used to monitor endogenous miR-132 activity in HEK293T cells (gray). The response for endogenous miR-132 was confirmed by transfection of 50 μM of 2′OMe miR-132 antisense inhibitor.

1. Magill ST, et al. (2010) microRNA-132 regulates dendritic growth and arborization of newborn neurons in the adult hippocampus. *Proc Natl Acad Sci USA* 107(47):20382–20387.

sample	date	sequencing lane	condition	total reads	uniquely mapped reads	% mapped
4	9/30/2011	1	miR-132	49238950	38751139	78.7%
8	9/16/2011	2	miR-132	47874130	36232555	75.7%
12	9/25/2011	3	miR-132	59463409	31767959	53.4%
3	9/30/2011	1	miR-124	28298431	22870389	80.8%
7	9/16/2011	2	miR-124	37706512	28860734	76.5%
11	9/25/2011	3	miR-124	30225288	22920129	75.8%
2	10/7/2011	1	miR-181d	48720171	30990325	63.6%
6	9/16/2011	2	miR-181d	36589447	28120433	76.9%
10	10/7/2011	3	miR-181d	37560483	28389637	75.6%

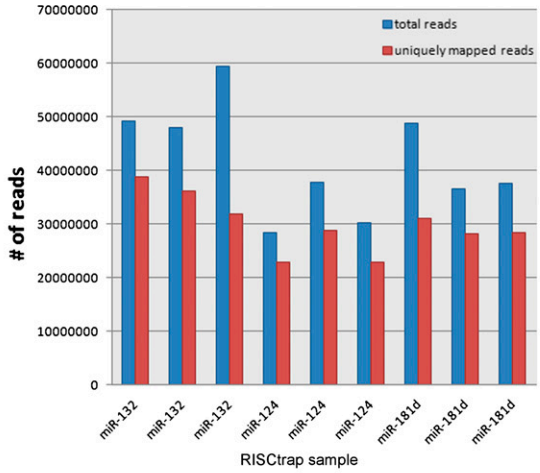

Biological replicate	1	2	3
Samples	**miR132_4**	**miR132_8**	**miR132_12**
Total uniquely mapped reads	38,478,115	35,804,620	36,479,358
Reads in exons	33,061,256	33,065,147	33,549,896
% of total	85.9%	92.3%	92.0%
Reads in introns	3,577,655	1,469,670	1,612,167
% of total	9.3%	4.1%	4.4%
Reads in intergenic regions	1,839,204	1,269,803	1,317,295
% of total	4.8%	3.5%	3.6%

Samples	**miR124_3**	**miR124_7**	**miR124_11**
Total uniquely mapped reads	22,664,502	28,530,994	22,538,531
Reads in exons	20,202,066	26,312,784	19,362,634
% of total	89.1%	92.2%	85.9%
Reads in introns	1,437,218	1,174,842	2,155,946
% of total	6.3%	4.1%	9.6%
Reads in intergenic regions	1,025,218	1,043,368	1,019,951
% of total	4.5%	3.7%	4.5%

Samples	**miR181d_2**	**miR181d_6**	**miR181d_10**
Total uniquely mapped reads	36,658,080	27,768,337	27,977,108
Reads in exons	33,686,188	25,354,161	25,835,534
% of total	91.9%	91.3%	92.3%
Reads in introns	1,551,797	1,406,986	1,131,829
% of total	4.2%	5.1%	4.0%
Reads in intergenic regions	1,420,095	1,007,190	1,009,745
% of total	3.9%	3.6%	3.6%

Fig. S2. Percentage of uniquely mapped reads for each RISCtrap sample and their distribution among exonic, intronic, and intergenic regions. On average, 40–50 million 100-bp single reads were obtained per RISCtrap sample and ~75% were uniquely mapped using Top Hat, a human GRCh37/hg19 reference genome, and RefSeq gene annotation guidance (as of Oct. 9, 2011). The distribution of these uniquely mapped reads among exonic, intronic, and intergenic regions is shown at the *Bottom*.

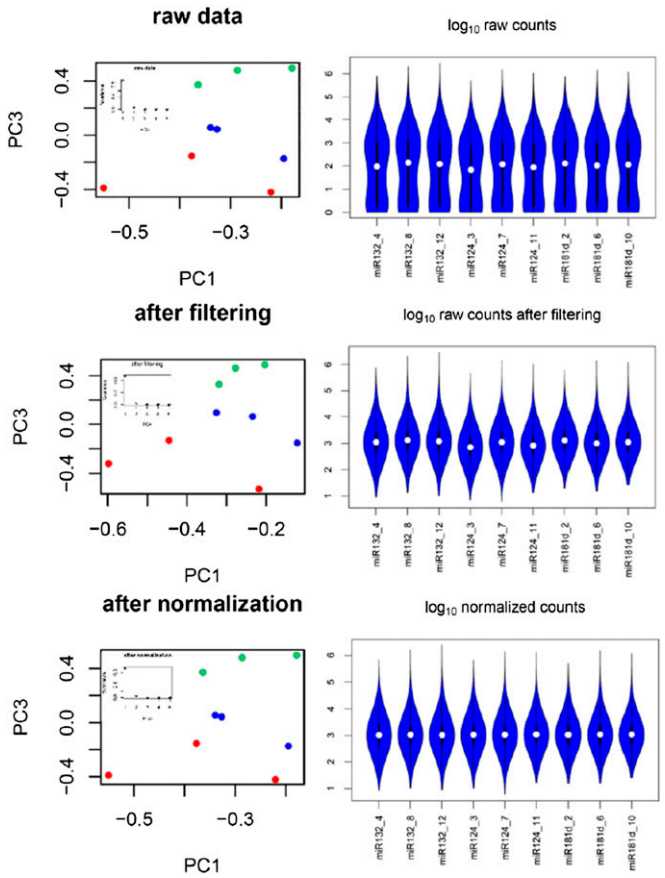

Fig. S3. Baseline minimum cutoff, normalization, and PCA of RISCtrap samples. To reduce the data dimensionality, we used principal components analysis (PCA) to transform a set of correlated variables into a smaller set of uncorrelated variables. PCA is useful for identifying patterns in the data and clustering datasets with similar conditions. The first component (PC1) describes the largest contribution to variability in the original data, whereas the second component (PC2) describes the next largest contribution to variability, etc. Read counts were assigned to each gene according to the RefSeq annotation. Non-polyadenylated genes and targets with read counts less than 200 across all samples were bioinformatically filtered (~11,800 targets) (*Middle*). The median of the geometic mean of the remaining 10,885 genes was then used for normalization (*Bottom*). At each step, datasets were analyzed by PCA to ensure that the clustering characteristics were maintained (*Left*). Meanwhile, violin plots were used to visualize the data shape and distribution (*Right*).

Pearson pairwise correlation	coefficient
mir132_4 vs mir132_8	0.82
mir132_4 vs mir132_12	0.76
mir132_8 vs mir132_12	0.99
mir124_3 vs mir124_7	0.82
mir124_3 vs mir124_11	0.79
mir124_7 vs mir124_11	1.00
mir181_2 vs mir181_6	0.87
mir181_2 vs mir181_10	0.87
mir181_6 vs mir181_10	1.00

Fig. S4. Pearson pairwise correlation coefficients among replicates. The Pearson pairwise correlation coefficients among replicates averaged above 0.80, suggesting high reproducibility among biological replicates for the RISCtrap assay.

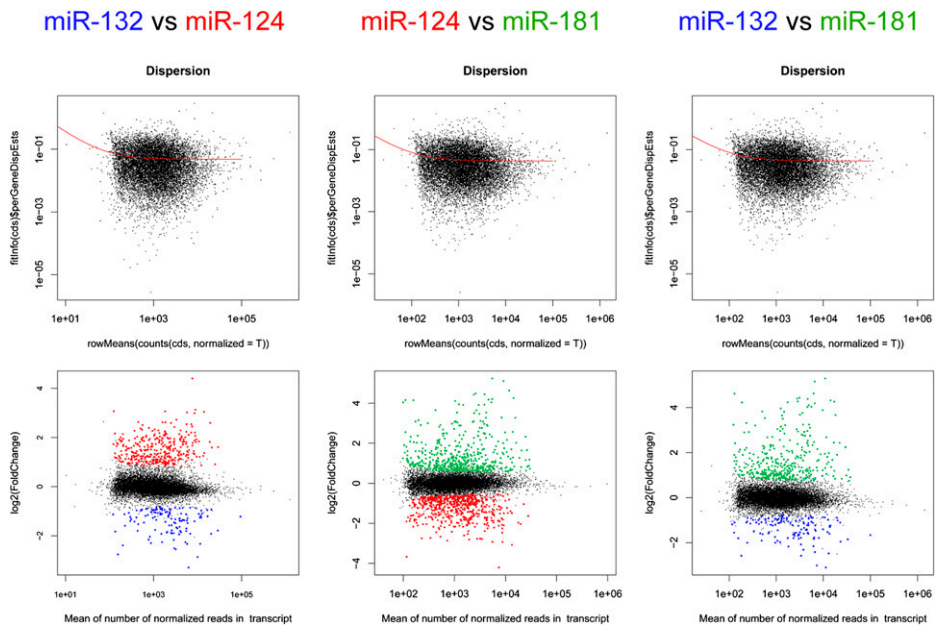

Fig. S5. Estimation of variance and differential enrichment for pairwise comparisons. The relationship between the data variance (dispersion) and mean is estimated in DESeq (1). Empirical dispersion values (black dots) were plotted against the normalized mean values per gene, with the fitted dispersion plotted as a red line (*Upper*). Differential enriched genes in pairwise comparisons were determined by ANOVA within the DESeq package, and significantly enriched genes were plotted as red, green, or blue dots in the corresponding graphs (*Lower*).

1. Anders S, Huber W (2010) Differential expression analysis for sequence count data. *Genome Biol* 11(10):R106.

a

	# of shared targets	contains ≥1 MRE for both microRNAs	contains MREs for miR-181 only	contains MREs for miR-124 only	contains MREs for miR-132 only	contains 0 MREs
miR-124 and miR-181	12	11	1	0	nd	0
miR-132 and miR-181	3	3	0	nd	0	0
miR-132 and miR-124	7	4	nd	1	1	1

b

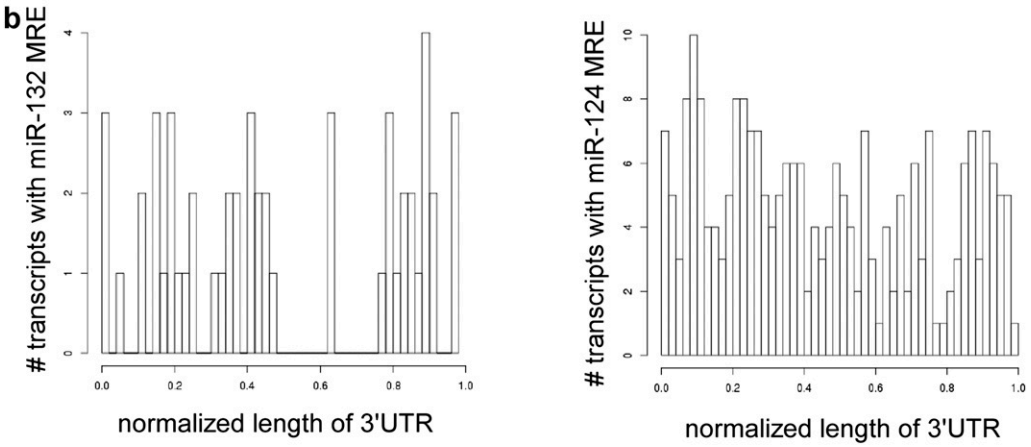

Fig. S6. Presence of MRE motifs among predicted coregulated targets and distribution along the length of normalized 3′UTRs. (*A*) Target sequences predicted to be coregulated by two distinct miRNAs were examined for inclusion of MRE motifs corresponding to both miRNAs. ND, not determined. (*B*) The frequency of MRE motifs is plotted against the relative position of MRE in the 3′UTR (miR-132, *Left*; miR-124, *Right*).

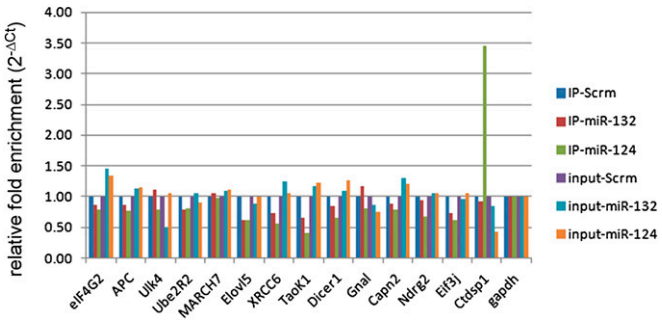

Fig. S7. Assessment of miR-124 targets not identified by RISCtrap for binding to RISC. Thirteen transcripts were selected for examination by qPCR for co-purification with RISC containing a scrambled miRNA, miR-132, and mir-124 in the presence of Flag–dnGW182. Input RNA (100 ng) was also analyzed to confirm that the transcripts were expressed in HEK293T cells. qPCR primers for Ctdsp1 and Gapdh were included as positive and negative controls, respectively. Values were normalized to Gapdh.

Other Supporting Information Files

Dataset S1 (XLSX)
Dataset S2 (XLSX)